1999

Classification of Torbanite and Cannel Coal. I. Insights from Petrographic Analysis of Density Fractions.

Zhiwen Han
Southern Illinois University Carbondale

Michael A. Kruge
Montclair State University, krugem@mail.montclair.edu

John C. Crelling
Southern Illinois University Carbondale

David F. Bensley
Southern Illinois University Carbondale

PREPRINT: Han Z., Kruge M. A., Crelling J. C., and Bensley D. F. (1999) Classification of torbanite and cannel coal. I. Insights from petrographic analysis of density fractions. *International Journal of Coal Geology* **38**:161-202.
https://doi.org/10.1016/S0166-5162(98)00013-5

Classification of torbanite and cannel coal. I. Insights from petrographic analysis of density fractions.

Zhiwen Han[1], Michael A. Kruge, John C. Crelling, and David F. Bensley[2]

Department of Geology, Southern Illinois University, Carbondale, IL 62901-4324 USA
[1]Pres. address: Deltech Engineering, 2893 E. La Palma Ave., Anaheim, CA 92806 USA
[2]Pres. address: Carbon Consultants International, Inc., Box 819, Carbondale, IL 62903 USA

Abstract

Torbanite and cannel coal are considered to be coals because of their low mineral content and overall physical morphology. However, the texture and composition of the organic matter in torbanite and cannel coal are similar to the kerogen occurring in oil shales and lacustrine source rocks. Therefore, understanding the nature and origin of organic components in torbanite and cannel coal is of significance in the study of kerogen and petroleum formation. In this research, a set of torbanites and cannel coals from different locations throughout the world were petrographically characterized and processed using a density gradient centrifugation (DGC) technique. Microscopically, the torbanite and cannel coal are composed of coarser maceral particles set in a fine-grained to amorphous groundmass. The groundmass is a mixture of more than one type of substance and accounts for 10 to 80% (by volume) of the torbanites and cannel coals. *Botryococcus*-related alginite is the most characteristic component of the torbanite. While sporinite typically is the main phytoclast in the cannel coals, in most cases the groundmass is volumetrically the dominant component, determining the overall character of the sample. This observation calls into question the traditional practice of classifying such coals using the alginite to sporinite ratio. Variations in composition, texture and fluorescence permits the recognition of three different types of groundmass: lamalginitic, bituminitic and vitrinitic. High purity alginite, sporinite, vitrinite and varieties of groundmass were separated using the DGC technique. The distribution of density fractions closely reflects the petrographic composition of the various torbanites and cannel coals. Distinct peaks on the density profiles represent the major organic components and peak magnitudes are functions of the percentage of the components, demonstrating that the density gradient profiles can be used to distinguish the different types of torbanite and cannel coal. The separation data also indicate a gradual shift towards higher density from lamalginitic to bituminitic to vitrinitic groundmass.

Keywords: torbanite, cannel coal, sapropelic coal, maceral, organic groundmass, organic petrology, density separation

1. Introduction

Traditionally, torbanite (also called boghead coal) and cannel coal are considered as end members in coal classification schemes on the basis of their relatively low ash yields. They are distinguished from humic coals by their uniform, compact fine-grained texture, and non-banded appearance. Their overall liptinite-rich composition and oil-prone nature also allow them to fit the definition of oil shales and source rocks. During the period of industrialization in Europe they were important fuel sources. Today, research related to torbanite and cannel coal has been focused on understanding the nature and origin of their organic components, which is useful in the study of kerogen and petroleum formation.

The organic matter in oil shales and source rocks is also divided into two categories, the structured (distinct macerals) and amorphous (groundmass) components. Due to the low concentration of organic matter, the observation and classification of the organic matter in source rocks have mainly been based on the chemically or mechanically concentrated kerogens (Burgess, 1974; Mukhopadhyay *et al.*, 1985; Thompson-Riser and Dembicki, 1986; Sentfle *et al.*, 1987). In contrast, the naturally high concentration of organic matter in torbanite and cannel coal gives them an inherent advantage as samples for conducting in-situ petrographic study on whole rocks, without the disruption caused by kerogen isolation and concentration in the laboratory.

As with the kerogen of oil shales and source rocks, the organic components of torbanite and cannel coal are divided into the distinct maceral particles and the fine-grained to amorphous groundmass. Previous studies related to torbanite and cannel coal have been focused on understanding the optical and chemical properties of the structured macerals, especially the *Botryococcus*-related alginite (for instance: Bertrand and Renault, 1892; 1893; Zalessky, 1914; Thiessen 1925; Blackburn and Temperley, 1936; Dulhunty, 1951; Maxwell *et al.*, 1968; Cane and Albion, 1971; Largeau *et al.*, 1984; Kalkreuth and Macauley, 1986; Hutton, 1987; Püttmann and Kalkreuth, 1989; Gentzis and Goodarzi, 1991). However, the groundmass has only been discussed separately in a few cases (Given *et al.*, 1985; Hower *et al.*, 1986; Hook and Hower, 1988; Hower, 1989; Han *et al.*, 1995). Our knowledge of the groundmass has been limited and unsystematic. Therefore, understanding the properties of the groundmass is one major focus of this paper, in addition to the petrography of the torbanite and cannel coal.

The second objective of this research was to separate the petrographic entities occurring in torbanite and cannel coal using density gradient separation (DGC). The DGC technique was first used for maceral separation of humic coals in the early 1980's (Dyrkacz and Horwitz, 1982; Dyrkacz *et al.*, 1984; Winans and Crelling, 1984). With recent advances in sample pre-treatment and centrifugation procedures, the DGC technique can be applied to any type of sedimentary organic matter, including torbanite (Han *et al.*, 1995) and source rock kerogens (Crelling, 1988; 1989; 1994; Taulbee *et al.*, 1991; Stankiewicz *et al.*, 1994; 1996).

2. Experimental methods

A total of 15 samples were used in this study, most of them from the collection of the Department of Geology, Southern Illinois University at Carbondale. This set of samples ranges from Ordovician to Jurassic in geological age, from sites in Asia, Africa, Australia, Europe and North America (Table 1).

Petrographic analyses including maceral analysis, reflectance measurements in oil and photomicrography, were performed using a Leitz MPV II microscope, equipped with both white light and blue light illumination systems. Sample preparation and petrographic analyses were conducted in accordance with standard ASTM procedures (ASTM, 1987). All whole coal samples were mechanically crushed to <850 μm, for a purpose of pellet-making. For each sample (whole coal and fractions), two pellets were made. For quantitative analysis, 500 points were counted on each of the pellets and the results averaged.

Splits of the crushed samples (<850 μm) were further ground to less than 75 μm size in a ball mill and then extracted with CH_2Cl_2 in a sonicator. The extraction residues were treated with 20% HCl for 24 hours and then with 30% HF for the same time period.

Following this acid demineralization, cryogenic treatment was performed by immersing the sample powders in liquid nitrogen so that fractures along maceral boundaries could be induced, due to the different expansion and contraction capacities of the various macerals. Micronization was accomplished with a Garlock FMT jet mill in a nitrogen atmosphere. It was found that the cryogenic treatment significantly enhanced the efficiency of micronization (Stankiewicz *et al.*, 1994; Han, 1995). The micronized samples were separated into a series of density fractions spanning a density range from 1.0 to 1.5 g/mL using an aqueous solution of CsCl with a Beckman J2-21M centrifuge in accordance with published DGC procedures (Dyrkacz and Horwitz, 1982; Dyrkacz *et al.*, 1984, Crelling, 1988). A representative split from each collected density fraction was made into pellets and examined with the reflected light microscope.

Rock-Eval pyrolysis was performed using a Rock-Eval II (Delsi, Inc.) in accordance with the procedures presented by Peters (1986). Two parameters, the T_{max} and Hydrogen Index (HI), are shown in Table 1.

3. Results and discussion

3.1. Petrographic composition

In hand specimen, torbanite and cannel coal are distinguished from humic coals by a uniform and non-banded appearance, commonly displaying conchoidal fractures. Microscopically, they possess a clastic texture with roughly equal-sized coarser maceral particles set in a fine-grained to amorphous groundmass (Han and Crelling, 1993). The major distinct macerals of the torbanite and cannel coal include alginite, sporinite and detrital vitrinite and inertinite. Minor amounts of resinite and cutinite are also often present. The groundmass content varies from a few percent up to 80%. Under the microscope, the torbanite and cannel coal are characterized by microstratifications, as shown by the parallel orientation of the elongate maceral particles and lamination of the groundmass.

The distinct macerals in torbanites and cannel coals generally fit the classical definitions of coal petrology (Stach *et al.*, 1982). *Botryococcus*-related alginite is the major maceral in the torbanite and commonly occurs in cannel coal as a minor component. The *Botryococcus*-related alginite is the only alginite occurring as a coarser maceral in the 15 samples used in this study. The *Botryococcus*-related alginite is further divided into two types: *Pila* and *Reinschia* (Bertrand and Renault, 1892 and 1893). Both *Pila* and *Reinschia* alginite are colonies of single cup-shaped cells. *Reinschia* has a spherical shell surrounding a comparatively large central cavity (Plate 1-A and D). *Pila* has a more solid form, the central cavity being either very small or absent, showing a fan-like structure with diverging radii (Plate 1-G and J, Plate 2-B and E). Therefore, the *Pila* alginites are usually smaller than the *Reinschia*.

Sporinites are the most important structured maceral in the cannel coals and are also often encountered in torbanites. Miospores are very common, scattered in the groundmass or between other maceral particles, showing a general orientation parallel to the bedding planes (Plate 1-J, Plate 2-A, B, E and H). Megaspores and sporangia were occasionally observed. Vitrinite occurred either as uniform lamellae (Plate 1-G, Plate 2-H) or, commonly, as irregular particles. Inertodetrinite (Plate 2-B and H) is very common and fragments of fusinite, semifusinite and macrinite are observed as well.

As shown in Table 1, the groundmass dominates most of the cannel coals and occurs as a major component in torbanites. Microscopic examination indicated that the groundmass is generally a mixture consisting of amorphous organic matter, micrinite and debris of various macerals, as well as some finely dispersed minerals (usually clay). Based on the variation of composition, texture, and fluorescence, three different types of groundmass are recognized in the 15 samples examined. Generally, in a given torbanite or cannel coal only one type of groundmass is seen.

3.1.1. Type 1: Lamalginitic groundmass

The lamalginitic groundmass is composed of densely packed lamellae (usually 0.1-0.2 mm thick) and characterized by a bright yellow to brown fluorescence (Plate 1-G and I). But the fluorescence is relatively weak compared to the co-occurring *Botryococcus*-related alginite. Under white light, it has a greenish to dark gray color and the lamellae become indistinguishable. Small amounts of micrinite, very fine inertodetrinite and comminuted clay are also included. The lamalginitic groundmass occurs in the Breckinridge Cannel of Kentucky (sample 8), and has been previously termed "bituminite groundmass" and considered to be derived from a variety of algal, bacterial, and faunal sources (Hower, 1989). Chemical analyses showed that the lamalginitic groundmass has a highly aliphatic nature (Han, 1995). Morphologically, it is somewhat similar to the layered lamalginite occurring in oil shales (Hutton, 1987, Cook and Sherwood, 1991), but different from the typical discreet lamalginite such as that seen in Rundle oil shale of Queensland, Australia (Hutton, 1987). In the Breckinridge sample, the individual lamellae appear to have been fused together and collectively occur as a groundmass surrounding the discrete maceral particles, such as *Botryococcus*-related alginite and vitrinite (Plate 1-G). Transition from the bright lamellae to a darker bituminitic material is also common. We propose that this groundmass type be called "lamalginitic", meaning essentially lamalginite occurring as groundmass.

3.1.2. Type 2: Bituminitic groundmass

Bituminitic groundmass is the most common groundmass type seen in this sample set, occurring in both torbanite and cannel coal. It is similar to the maceral bituminite, with its low reflectance, moderate brownish fluorescence and lack of any characteristic shape. Bituminite was first defined by Teichmüller (1974) as a liptinite maceral that occurs in coals, oil shales and source rocks. Later, Teichmüller and Ottenjann (1977) divided bituminite into three types which cover amorphous organic substances from brightly fluorescing to almost non-fluorescing. Based on our observations, the "bituminite" in the torbanite and cannel coal is an amorphous bituminitic material, commonly mixed with tiny yellow fluorescing lamellae, micrinite, debris of various distinct macerals and finely-dispersed clay. The parallel orientation of the embodied elongated maceral particles such as microspores and inertodetrinite give the groundmass an overall layered appearance.

When the bituminitic material is dominant, it has an overall uniform appearance. With blue light illumination, it showed a moderate reddish to brown fluorescence. Under white-light, it is a dark gray amorphous organic matter, interspersed with micrinite and clay particles. Typical examples are observed in the Australian Middle River torbanite (sample 2, Plate 1-D, F), Australian Joadja torbanite (sample 4), the Scottish torbanite (sample 6), and the Chinese torbanite (sample 7).

In some cases, the bituminitic groundmass contains many tiny (2-3 μm) lamellae with a yellow fluorescence, resulting in a filamentous texture. These microlamellae are generally oriented along bedding planes (Plates 1-J, 2-A). Under white light, the microlamellae are indistinguishable from the bituminitic material. Due to the incorporation of micrinite and clay particles, the groundmass is seen as a dark gray to black substance with a fine-grained appearance under white light. The microlamellae are smaller than the co-existing microspores and also the lamellae in lamalginitic groundmass. However, the yellow fluorescence of microlamellae suggests that they are possibly derived from algal or other liptinitic material. Typical examples are seen in sample 9 (Kane County, Utah), sample 10 (Plate 2-A, the Kentucky cannel coal) and sample 13 (Plate 1-J, Kanawha, West Virginia).

The bituminitic groundmass always contains micrinite. Micrinite has been defined as an inertinite maceral (Stach *et al.*, 1982). It is characterized by the rounded shape and the very small size of its grains, which are commonly about 1 μm across. In some cases, the micrinite is so abundant in the bituminitic groundmass that the whole groundmass showed a whitish gray color and a micrinitic texture under white light illumination, as seen in sample 11 (Plate 2-B and D) and sample 12. Under blue light, the groundmass has a moderate reddish to brown fluorescence. In an extreme case, other researchers reported a groundmass as "being seen to consist of approximately 90% micrinite accompanied by finely detrital vitrinite, inertinite and liptinite particles and trace of bituminite" (Hook and Hower, 1988). Therefore, Hook and Hower (1988) called such groundmass "micrinitic". However, in our sample set, we observed a compositional continuum, with bituminitic groundmass composed of varying proportions of bituminite, microlamellae and micrinite.

3.1.3. Type 3: Vitrinitic groundmass

Under white light, vitrinitic groundmass appears similar to desmocollinite in humic coals, with its gray color and groundmass morphology. It is also associated with dispersed micrinite, clay, and debris of various maceral particles. With blue-light illumination, it shows a dark reddish-brown fluorescence (Plate 2-E and G), which is weaker than that of other types of groundmass. Vitrinitic groundmass is the dominant constituent in a cannel coal from Linton, Ohio (sample 14).

3. 2. Types of Torbanite and Cannel Coal

As shown in Fig. 1, the samples can clearly be divided into two major groups: torbanites (samples 1 to 7), which contain large amounts of alginite, and cannel coals (samples 8 to 15), in which sporinite and groundmass are the most significant. The Rock-Eval Hydrogen Indices (HI) of the torbanite generally increase with increasing alginite content (Table 1, Fig. 1), whereas the HI of cannel coals is proportionately related to both sporinite and groundmass contents (Table 1).

In the torbanite category, *Botryococcus*-related alginite is the most characteristic component. Sporinite and detrital vitrinite and inertinite also occur. Bituminitic groundmass is the most common type in torbanite. The seven torbanite samples show a compositional continuum, with alginite content decreasing as groundmass content increases (Fig. 1).

Three of the samples (Fig. 1) are extremely rich in alginite, including the Australian Alpha torbanite (sample 1) and Middle River torbanite (sample 2), as well as the South African torbanite (sample 3). Only minor amounts of sporinite, vitrinite and inertinite are present. The groundmass occupies the spaces between the alginite and other maceral particles, showing a typical "particle-supported" texture (Plate 1-A and D). Their Rock-Eval Hydrogen Indices are very high, giving 848 mg HC/g TOC for sample 1 and 838 mg/g for sample 2 (Table 1).

Samples with moderate alginite content include the Joadja torbanite (sample 4), the Cannelburg torbanite (sample 5) and the classical Scottish torbanite (sample 6). *Botryococcus*-related alginite is still the dominant component (about 40% of the total volume). The groundmass (30 to 40% of the total volume) is more abundant than in samples 1,2 and 3, as are sporinite, vitrinite and inertinite (Fig. 1). The Hydrogen Indices vary between 507 and 666 mg/g (Table 1).

Sample 7 (Shanxi, China) is distinguished by its relatively low alginite content (21%) and the dominance of the groundmass (52%). On the basis of the alginite to sporinite ratio, it falls into the cannel boghead category in the classification system of Bertrand and Renault (1892; 1893). It contains relatively larger amounts of higher plant derived macerals such as sporinite and vitrinite (Table 1). The Hydrogen Index (471 mg/g) is correspondingly low.

In contrast, cannel coals in the sample set contain little or no alginite. The alginite that does occur is usually structureless (Plates 1-G, 1-J, 2-E). Instead, sporinite is typically the most characteristic phytoclast and the groundmass usually dominates volumetrically (Table 1, Fig. 1).

The Kentucky Breckinridge cannel (Sample 8, Plate 1-G) and the Utah King cannel (sample 9) are very similar petrographically (Table 1 and Fig. 1). The Breckinridge cannel has been well documented by Hower *et al.* (1986) and Hower (1989), and the King cannel was previously studied by Given *et al.* (1985). Both of them are strongly dominated by groundmass. Vitrinite (often layered) is the most abundant coarse-grained maceral, while sporinite contents are low. In addition, they contain a few percent *Botryococcus*-related alginite and inertodetrinite. In the King cannel, about 2% of the total volume is resinite. However, the two samples are distinguished by their groundmass types. The groundmass contained in the Breckinridge cannel is the brightly fluorescing lamalginitic type (Plate 1-G). Due to the predominance of such a highly aliphatic groundmass (Han, 1995), the Hydrogen Index (620 mg HC/g TOC) is the highest of any cannel coal in this sample set (Table 1). The groundmass occurring in the King cannel is basically a bituminitic type, containing abundant microlamellae. The Hydrogen Index of the King cannel is 434 mg/g.

Samples 10-14 display the typical features of cannel coals. In hand specimen, they are uniform, compact and well indurated. Microscopically, sporinite is the most significant phytoclast (10-20%), and bituminitic groundmass is the dominant constituent (about 60-70%). They also contain significant amounts of detrital vitrinite and inertinite (2 to 13%). *Botryococcus*-related alginite is common, but rarely exceeds 5% (Plate 1-J, Plate 2-B and E). The Hydrogen Indices are only moderately high, varying between 351 and 409 mg/g.

The most unusual sample is the Devonian cannel coal (sample 15) from Melville Island in the Canadian Arctic. It has a simple petrographic composition, consisting almost solely of sporinite and structureless vitrinite (Plate 2-H). It is well-known for its high sporinite content (Gentzis and Goodarzi, 1991; Goodarzi and Goodbody, 1990). The sporinite particles are often grouped as layers or lenses. According to Gentzis and Goodarzi (1991), the Melville cannel coal is generally uniform and compact in hand specimen. But the sample studied in this paper has a banded-texture, due to alternation of the sporinite-rich and vitrinite layers, and thus the hand specimen is very fragile. Because of the high sporinite content (65 %), its Hydrogen Index (579 mg/g) is higher than that seen for most of the other cannel coals (Table 1).

3.3. Density Gradient Centrifugation

Fig. 2 shows the density gradient profiles of the 15 torbanites and cannel coals. A density gradient profile is a plot of the recovered weight of the density fractions as a function of density, normalized to the maximum. The numbered fractions are those chosen for petrographic evaluation for purity, the results of which are presented in Table 1. Because of the high concentration of liptinite macerals, the DGC fractions of torbanite and cannel coal mainly fall in a density range from 1.0 to 1.3 g/mL, which is clearly less than the density range (1.2 to 1.6 g/mL) typical of humic coals (Crelling, 1988; 1989; 1994).

3.3.1. Torbanites

Fig. 2A to 2G display the density gradient profiles of the torbanites (samples 1 to 7), which are arranged by decreasing alginite content. All the density gradient profiles of torbanites are characterized by two distinct peaks: one peak representing the *Botryococcus*-related alginite at 1.0 - 1.10 g/mL and another at about 1.15 to 1.25 g/mL predominantly groundmass. From 3A to 3G, the left peak (alginite) generally declines with decreasing alginite content as the right (groundmass) becomes larger with increasing groundmass.

Each of the density gradient profiles of the three alginite-dominated torbanites (samples 1 to 3) has a very strong alginite peak (Fig. 2A to 2C). The groundmass peak is very weak or non-existent. With samples 1 and 2, the alginite could not be separated completely using the regular DGC procedures due to overloading at densities below 1.1 g/mL. A better separation was obtained by performing repeat DGC runs using high resolution procedures (Han *et al.*, 1995), in which the alginite was pre-concentrated by float/sink treatment prior to DGC. Fractions 39 and 40 (sample 1) and 36 and 38 (sample 2) are from high resolution DGC runs (Table 1).

In Fig. 2D to 2F, both the alginite and groundmass peaks are prominent, reflecting the dominance of both alginite and groundmass in samples 4, 5 and 6. Sample 4 was previously discussed in detail (Han *et al.*, 1995). In the density gradient profile of the Chinese torbanite (sample 7), the groundmass peak is shown to be much stronger than the alginite peak (Fig. 2G), corresponding to the high concentration of groundmass (52 %) and relatively lower alginite content (21 %).

3.3.2. Cannel coals

Fig. 2H to 2O are the density gradient profiles of the 8 cannel coals (samples 8 to 15). Unlike the torbanite density gradient profiles, which are characterized by a bimodal pattern, most of the density gradient plots of the cannel coals show only a single strong peak. This peak is mainly due to groundmass, consistent with its predominance (60-80%) in most cannel coals in the sample set. The groundmass peak varies in density from 1.10 to 1.32 g/mL. Sporinite is shown as a distinct peak (1.15 to 1.23 g/mL) only in the profiles of the Linton cannel (sample 14, Fig. 2N) and the Canadian Melville cannel (sample 15, Fig. 2O), being especially prominent in the latter case.

3.3.3. Purity of maceral concentrates

The density gradient profiles of torbanites and cannel coals (Fig. 2) and maceral analysis of the density fractions (Table 1) indicate that only the dominant components (alginite, sporinite, vitrinite and the varieties of groundmass) could be separated. The minor components, such as cutinite and inertinite, are found in fractions collected between or beside the major peaks. The density ranges of the separated macerals and groundmass are summarized in Fig. 3.

Botryococcus-related alginite was the least dense maceral, with a density range of 1.02 to 1.10 g/mL. High purity alginites (92-99 %) were obtained from all the seven torbanite samples (Table 1). Microscopic examination indicates that only small groundmass pieces are attached to the edge of alginite (Plate 1B and E). The alginite concentrate separated from Kentucky Breckinridge cannel (sample 8) is only 83 % pure (Table 1, Plate 1H).

The sporinite generally fell in a density range of 1.14 to 1.23 g/mL (Fig. 3). High purity sporinite fractions (92-99 %) were obtained from the West Virginia cannel (sample 13, Plate 1K), the Ohio Linton cannel (sample 14, Plate 2F) and the Canadian Melville cannel (sample 15, Plate 2I). In the density gradient profiles of these three cannel coals, the sporinite fractions appear as either a distinct peak or shoulder (Fig. 2M-O). But sporinite was not completely separated from the groundmass in samples 5, 11 and 12 (Fig. 2E, K, L). For these three samples, the cleanest sporinite obtained is only about 70 to 75% pure (Plate 2C).

High purity vitrinite was separated only from the Canadian Melville Island cannel (sample 15, Plate 2J) and it appears as a distinct peak at 1.28-1.33 g/mL (Fig. 2O). The density range of the vitrinite concentrates are generally consistent with those (1.28-1.35 g/mL) separated from typical humic coals (Crelling, 1988 and 1989, Kruge and Bensley, 1994). A fraction predominantly composed of degraded vitrinite (about 84%) was obtained from the Australian Alpha torbanite (sample 1, Plate 1- C). It has a density around 1.24 g/mL and a dark gray, uniform appearance.

3.3.4. Purity of groundmass concentrates

A variety of groundmass types were separated from most of the samples, except from the Alpha torbanite and Melville cannel coal (Samples 1 and 15), in which groundmass is only a minor constituent. Generally, the groundmass falls in density range of 1.12 to 1.33 g/mL (Fig. 3), lying between the *Botryococcus*-related alginite and vitrinite, and overlapping with sporinite. In most cases, the separation results were satisfactory, with purity above 90% (Table 1, Plates 1 and 2). It should be mentioned that, due to the fluorescence of the mounting material, the groundmass in the concentrates appears darker than that in the blue light photomicrographs of the bulk samples.

It is interesting to note that the density of groundmass can be correlated with its petrographic properties. The brightly fluorescing lamalginitic groundmass (Plate 1G, I) has a relatively low density of 1.12 to 1.17 g/mL (Fig. 2H), while the higher density of the vitrinitic groundmass (1.28-1.31 g/mL, Plate 2E, F) is very close to that of the vitrinite maceral. In general, the groundmass exhibits a gradual shift toward higher density from lamalginitic to bituminitic to vitrinitic (Fig. 3).

In summary, the DGC separation data of torbanite and cannel coals are consistent with petrographic composition. The sensitivity of the DGC profiles to the compositional variability of torbanites and cannel coals demonstrates that density profiling can be used as a diagnostic tool to distinguish not only torbanite and cannel coal from humic coal and from each other, but also between the varieties of torbanite and cannel coal. In recent years, density gradient centrifugation has been used as a separation tool. In this research, the first systematic separation of torbanite and cannel coal has revealed the value of the DGC technique in characterization and differentiation of various types of sedimentary organic matter.

3.4. Rank determination

Vitrinite reflectance is the most common petrographic parameter used in determination of the thermal maturity of sedimentary organic matter. However, reflectance suppression of the vitrinite contained in liptinite-rich rock types is ubiquitous (Hutton and Cook, 1980; Goodarzi and Goodbody, 1990; Gentzis and Goodarzi, 1991, Lo, 1993). This has increased the difficulty of maturity evaluation for oil and gas exploration. Therefore, it is necessary to consider other maturity parameters and the overall regional geothermal context in addition to vitrinite reflectance, while dealing with any liptinite-rich coals, oil shales or source rocks.

Solely based on the vitrinite reflectance measured on the torbanites and cannel coals, most of the samples in Table 1 would fall into the immature stage. A few would have just entered the mature stage, if 0.5% R_{max} is taken as the cutoff between mature and immature. However, the low vitrinite reflectance of those Carboniferous-Permian samples is clearly inconsistent with their regional coalification context. This inconsistency is directly demonstrated by the vitrinite reflectance data of five humic coals adjacent to the torbanites and cannel coals (Table 1). The maximum vitrinite reflectance measured on the adjacent humic coals is on the average 0.34% higher than that measured on the torbanite and cannel coal.

The Rock-Eval analysis shows that the T_{max} values of most of the samples fall between 436 and 456 °C (Table 1), which corresponds to a vitrinite reflectance of around 0.6-0.8% (Peters, 1986). The evidence for suppression of vitrinite reflectance and the Rock-Eval

T_{max} data together suggest that most of the torbanites and cannel coals in Table 1 had entered a maturity stage approximately equivalent to the high volatile bituminous coal rank.

4. Summary and conclusions

Microscopically, both the torbanite and cannel coal are composed of roughly equal-sized coarser maceral particles set in a fine-grained to amorphous groundmass. The major macerals are *Botryococcus*-related alginite, sporinite and detrital vitrinite and inertinite. Minor amounts of resinite and cutinite are also seen.

The groundmass accounts for 10 to 80% (by volume) of the torbanite and cannel coal. Based on composition, texture and fluorescence, three different types of groundmass are recognized: lamalginitic, bituminitic and vitrinitic. Generally, in a given torbanite or cannel coal only one type of groundmass is seen.

In torbanite, *Botryococcus*-related alginite is the most characteristic component and the bituminitic groundmass is common. Among the seven torbanite samples, alginite and groundmass contents vary considerably (and inversely). The alginite content is positively correlated with the Rock-Eval Hydrogen Index. In contrast, sporinite is the most important maceral phytoclast in most of the eight cannel coal samples, but the groundmass usually dominates. There is considerable variation in sporinite and groundmass content.

High purity *Botryococcus*-related alginite, sporinite, vitrinite and varieties of groundmass were isolated using density gradient centrifugation. The DGC data showed a gradual shift towards high density from lamalginitic, bituminitic to vitrinitic groundmass in a range of 1.12 to 1.32 g/mL.

The results show that there is a clear petrographic difference between the torbanite and cannel coal samples. The torbanites have more phytoclasts and less groundmass than the cannel coals. All have greater than 20% alginite and many are dominated by alginite. The cannel coals, on the other hand, usually have less than 20% sporinite as phytoclasts and are dominated by the groundmass. In as much as the samples studied are representative of cannel and torbanite coals, these results throw doubt on the validity of trying to classify these coals on their alginite/sporinite ratio. While the torbanites are almost always dominated by alginite, the cannel coals are almost always dominated by groundmass.

The results clearly show that the DGC technique has been successful in separating the phytoclasts from the matrix in all of these coals. In fact, concentrations suitable for showing chemical differences between the two components have been obtained. This is something that has never been demonstrated before on such a range of samples. The DGC results also show the different phytoclasts and groundmass types have different densities and, therefore, implies that they probably have different chemistries as well.

When the petrographic and DGC results are compared, the correspondence between the two types of data is remarkable. The maxima on the density profiles mark those fractions in which the phytoclast and matrix components are in high concentration. The DGC procedure not only provides samples of these individual components of the cannel and torbanite coals, but the density profile also provides reliable data on both the kinds and distribution of components in the samples.

As with other liptinite-rich organic matter types, the suppression of vitrinite reflectance is a common problem with torbanite and cannel coal. Reflectance corrections should be applied to such samples (about 0.3% R_{max} in this case) and other means of rank assessment should be employed.

Acknowledgments

We gratefully acknowledge the Rock-Eval analyses by Charlie Landis and ARCO and the contributions of samples by our colleagues, R. M. S. Falcon (Falcon Research Laboratory Ltd., South Africa), Fariborz Goodarzi (Geological Survey of Canada), James C. Hower, (Center for Applied, Energy Research, University of Kentucky), and Adrian Hutton (Department of Geology, University of Wollongong, Australia). We also wish to thank John E. Utgaard, Russell Dutcher, Harry Marsh, Stephen Palmer, Bill Huggett, Corliss Thies and Artur Stankiewicz for their technical assistance. The thoughtful comments of A. C. Cook and W. A. Hartgers helped to improve the final version of the manuscript.

References

American Society for Testing Materials (ASTM), 1987. Annual Book of ASTM Standards: Part 26: Gaseous Fuels; Coal and Coke; Atmospheric Analysis. ASTM, Philadelphia.

Bertrand, C. E., Renault, B., 1892. *Pila bibractensis* et le boghead d'Autun. Soc. hist. nat. Autun Bull. 5, 159-253.

Bertrand, C. E., Renault, B., 1893. *Reinschia australis* et premières remarques sur la kerosene shale de la Nouvelle-Galles du Sud. Soc. hist. nat. Autun Bull. 6, 321- 425.

Blackburn, K. B., Temperley, B. N., 1936. *Botryococcus* and the algal coals. Part I: A reinvestigation of the alga *Botryococcus Braunii Küzing*; Part II: Boghead controversy and the morphology of the boghead algae. Trans. Roy. Soc. Edinburgh 58(3), 841-854, 855-870.

Burgess, J. D., 1974. Microscopic examination of kerogen (dispersed organic matter) in petroleum exploration. Geological Society of America Special Paper 153, 69-87.

Cane, R. F., Albion, P. R., 1971. The phytochemical history of torbanites. Journal and Proceedings, Royal Society of New South Wales. 104, 31-37.

Cook, A. C., Sherwood, N. R., 1991. Classification of oil shales, coals and other organic-rich rocks. Org. Geochem. 17, 211-222.

Crelling, J. C., 1988. Separation and characterization of coal macerals including pseudovitrinite. Ironmaking Proceedings-AIME, Vol. 43, 351-356.

Crelling, J. C., 1989. Separation and characterization of coal macerals: Accomplishments and future possibilities. Am. Chem. Soc. Div. Fuel Chem. Prepr. 34 (1), 249-255.

Crelling, J. C., 1994. Targeting single coal macerals with density gradient centrifugation experiments. Am. Chem. Soc. Div. Fuel Chem. Prepr. 39(1), 13-17.

Dulhunty, J. A., 1951. Occurrence and origin of Australian torbanite. Oil Shale and Cannel Coal, 2, Institute of Petroleum, London, 155-161.

Dyrkacz, G. R., Horwitz, E. P., 1982. Separation of coal macerals. Fuel 61, 3-12.

Dyrkacz, G. R., Bloomquist, C. A. A., Ruscic, L., 1984. High-resolution density variations of coal macerals. Fuel 63, 1367-1374.

Gentzis, T., Goodarzi, F., 1991. Petrology, deposition environment and utilization potential of Devonian cannel coals from Melville Island, Canadian Arctic Islands. Bull. Soc. Geol. France 162**,** 239-253.

Given, P. H., Davis, A., Kuehn, D., Painter, P. C., Spackman, W., 1985. A multi- faceted study of a Cretaceous coal with algal affinities. I. Provenance of the coal samples and basic compositional data. Int. J. Coal Geol. 5, 247-260.

Goodarzi, F., Goodbody, Q., 1990. Nature and depositional environment of Devonian coals from western Melville Island, Arctic Canada. Int. J. Coal Geol. 14, 175-196.

Han, Z., 1995. Organic geochemistry and petrology of torbanite, cannel coal and their constituent macerals. Ph.D. thesis, Southern Illinois University at Carbondale, 235 p.

Han, Z., Crelling, J. C., 1993. Observations on the petrographic composition of cannel and boghead coals. Proc. 7th Int. Conf. on Coal Sci., Banff, Alberta, Canada, vol. 1, pp. 144-147.
Han, Z., Kruge, M. A., Crelling, J. C., Stankiewicz, B. A., 1995. Organic geochemical characterization of the density fractions from a Permian torbanite. Org. Geochem. 22, 39-50.
Hook, R. W., Hower, J. C., 1988. Petrography and taphonomic significance of the vertebrate-bearing cannel coal of Linton, Ohio (Westphalian D, Upper Carboniferous). J. Sediment. Petrol. 58, 72-80.
Hower, J. C., 1989. Petrology of liquefaction residues from the Breckinridge cannel, western Kentucky. Org. Geochem. 14, 299-305.
Hower, J. C., Taulbee, D. N., Poole, C., Kuehn, D. W., 1986. Petrology and Geochemistry of the Breckinridge seam - A torbanite from Western Kentucky. 1986 Eastern Oil Shale Symp. Proc., 267-280.
Hutton, A. C., Cook, A. C., 1980. Influence of alginite on the reflectance of vitrinite from Joadja, NSW, and some other coals and oil shales containing alginite. Fuel 59, 711-714.
Hutton, A. C., 1987. Petrographic classification of oil shales. Int. J. Coal Geol. 8, 203- 231.
Kalkreuth, W. D., Macauley, G., 1986. The organic petrology and geochemistry of carboniferous oil shales from Eastern Canada. 1986 Eastern Oil Shale Symp. Proc., 257-265.
Kruge, M. A., Bensley, D. F., 1994. Flash pyrolysis-gas chromatography/mass spectrometry of Lower Kittanning vitrinites: Changes in the distributions of polyaromatic hydrocarbons as a function of coal rank, in: Mukhophadyay, P.K., Dow, W.G. (Eds.), Vitrinite Reflectance as a Maturity Parameter: Applications and Limitations. American Chemical Society Symposium Series 570, pp. 136-148.
Largeau, C., Casadevall, E., Kadouri, A., Metzger, P., 1984. Formation of *Botryococcus*-derived kerogens — Comparative study of immature torbanites and of the extant alga *Botryococcus braunii*. Org. Geochem. 6, 327-332.
Lo, H. B., 1993. Correction criteria for the suppression of vitrinite reflectance in hydrogen-rich kerogens: preliminary guidelines. Org. Geochem. 20, 653-657.
Maxwell, J. R., Douglas, A. G., Eglinton, G., McCormick, A., 1968. The Botryococcenes--hydrocarbons of novel structure from the alga *Botryococcus braunii*, Kützing. Phytochem. 7, 2157-2171.
Mukhopadhyay, P. K., Hagemann, H. W., Gormly, J. R., 1985. Characterization of kerogens as seen under the aspects of maturation and hydrocarbon generation. Erdol Kohle, Erdgas, Petrochem. 38, 7-18.
Peters, K. E., 1986. Guidelines for evaluating petroleum source rock using programmed pyrolysis. AAPG Bull. 70, 318-329.
Püttmann, W., Kalkreuth, W., 1989. Comparison of hydrocarbon compositions in a sequence of humic coals, cannel coals and oil shales from the Pictou coalfield, Nova Scotia. Atlantic Geology 25, 93-103.
Senftle, J. T., Brown, J. H., Larter, S. R., 1987. Refinement of organic petrographic methods for kerogen characterization. Int. J. Coal Geol. 7, 105-117.
Stach, E., Mackowsky, M.-Th., Teichmüller, M., Taylor, G. F., Chandra, G., Teichmüller, R., 1982. Stach's Textbook of Coal Petrology. 2nd edition, Gebruder Borntraeger, Berlin. 535pp.
Stankiewicz, B. A., Kruge, M. A., Crelling, J. C., Salmon, G. L., 1994, Density gradient centrifugation: Application to the separation of macerals of Type I, II, and III sedimentary organic matter. Energy & Fuels 8, 1523-1521.

Stankiewicz, B. A., Kruge, M. A., Mastalerz, M., Salmon, G. L., 1996, Geochemistry of the alginite and amorphous organic matter from Type II-S kerogens. Org. Geochem. 24, 495-509.

Taulbee, D. N., Hower, J. C., Greb, S. F., 1991. Examination of micrinite concentrates from the Cannel City coal bed of eastern Kentucky: proposed mechanism of formation. Org. Geochem. 17, 557-565.

Teichmüller, M., 1974. Über neue Macerale der Liptinit-Gruppe und der Entstehung von Micrinit. Fortschr. Geol. Rheinld. Westfal. 24, 37-64.

Teichmüller, M., Ottenjann, K., 1977. Art und Diagenese von Liptiniten und lipiden Stoffen in einem Erdolmuttergestein auf Grund fluoreszenzmikroskopischer Untersuchungen. Erdol u. Kohle 30, 387-398.

Thiessen, R., 1925. Origin of the boghead coals. U. S. Geol. Surv. Prof. Papers, 132-I, 121-135.

Thompson-Rizer, C. L., Dembicki, H. Jr., 1986. Optical characteristics of amorphous kerogens and the hydrocarbon-generating potential of source rocks. Int. J. Coal Geol. 6, 229-249.

Winans, R. E., Crelling, J. C., 1984. Chemistry and characterization of coal macerals: overview, in: Winans R. E., Crelling J. C. (Eds.), Chemistry and Characterization of Coal Macerals, Am. Chem. Soc. Symp. Ser. 252, pp. 1-20.

Zalessky, M., 1914. On the nature of *Pila*, the yellow bodies of boghead, and on sapropel of the Ala-Kool of Lake Balkhash. Bull. Com. Geol., St. Petersburg, 33, 495-507.

Table 1. Petrographic and Rock-Eval data of the 15 torbanites, cannel coals and their density fractions. ID: sample number used in this study. SIU No.: Southern Illinois University coal sample collection serial number. R_{max} maximum vitrinite reflectance in oil. R_{max} humic coal: vitrinite reflectance measured on adjacent humic coal samples, if available. T_{max} and HI: Rock-Eval temperature of maximum pyrolysis yield and Hydrogen Index. Frac.: DGC fraction number (see Fig. 2). Density: density of DGC fraction. Alg.: alginite. Spo.: sporinite. Cut.: cutinite. Res.: resinite. Vitr.: vitrinite. Iner.: inertinite. GM: groundmass. The predominant groundmass type is lamalginitic in Sample 8, vitrinitic in Sample 14, and bituminitic in the rest.

ID	SIU No.	Location	Age	Rmax %	Rmax Humic Coal	Tmax (°C)	HI	Frac.	Density (g/mL)	Petrographic Composition (vol%) Alg.	Spo.	Cut.	Res.	Vitr.	Iner.	GM
1	2262	Alpha, Queensland	Permian	0.43		448	848	Whole		89	0.5			2.6	1.7	6.2
		Australia						11	1.369					13.6	66.6	19.8
								19	1.242		0.4			84.3		15.3
								27	1.104	69.4	2.5			3.5		24.6
								36	1.032	97.9						2.1
								39	1.026	99.0						1.0
								40	1.021	92.2						7.8
2	668	Middle River	Permian	0.39		456	838	Whole		76.7	1.4			4.2	3.9	13.8
		N.S.W., Australia						14	1.190	0.2	0.2				0.4	99.2
								15	1.181	0.6	0.2				0.2	99.0
								16	1.171	2.1	1.6				0.2	96.1
								32	1.037	96.6						3.4
								36	1.024	98.8						1.2
								38	1.021	99.6						0.4
3	2331	Transvaal	Permian	0.48				Whole		69.6	3.5			1.6	4.0	21.3
		South Africa						4	1.350		1.1			29.2	3.2	66.5
								8	1.288	5.7	3.6			16.2	2.2	72.3
								12	1.228	9.1	28.9			11.2		50.8
								27	1.043	99.2						0.8
								29	1.032	99.6						0.4
								31	1.025	99.8						0.2
4	670	Joadja	Permian	0.34		454	582	Whole		44.4	8.1	1		6.6	7.7	32.2
		N.S.W., Australia						18-19	1.195		0.2				0.2	99.6
								28-35	1.045	99.7						0.3
5	2248	Cannelburg	Westphalian	0.48		445	666	Whole		40.6	10.9	0.1	0.2	2	3.8	42.4
		Indiana, USA.						14	1.237	0.8	1.0			0.8	1.5	95.9
								18	1.186	1.0	3.1			1.2		94.7
								20	1.161	1.1	74.8					24.1
								26	1.091	57.8						42.2
								30	1.056	83.7						16.3
								33	1.039	92.4						7.6
6	1210	Torbane Hill	Westphalian	0.54		456	507	Whole		37.4	13.1			2.1	7.8	39.6
		Scotland, U.K.						9	1.235						0.2	99.8
								10	1.226		0.2				0.2	99.6
								11	1.217		0.2					99.8
								13	1.197	0.2	9.8					90.0
								23	1.095	84.6	0.8					14.6
								25	1.077	93.2						6.8
								26	1.068	95.8						4.2
								28	1.055	98.8						1.2
7	2244	Shanxi, China	Permian	0.52	0.77	453	471	Whole		21.4	6	1.1		8.1	11.6	51.8
								10	1.240						0.9	99.1
								12	1.221		0.2				0.2	99.6
								13	1.212		0.9					99.1
								25	1.086	97.0	0.4					2.6
								27	1.066	98.6						1.4
								28	1.058	99.6						0.4

Table 1. (continued)

ID	SIU No.	Location	Age	Rmax %	Rmax Humic Coal	Tmax (°C)	HI	Frac.	Density (g/mL)	Petrographic Composition (vol%) Alg.	Spo.	Cut.	Res.	Vitr.	Iner.	GM
8	646	Breckinridge	Westphalian	0.38	0.58	445	620	Whole		4.5	1.8			12.4	2.1	79.2
		Hancock Co.						14	1.184	0.2				3.5		96.3
		Kentucky, USA.						16	1.163	0.2				3.5		96.3
								18	1.144	0.4				1.5		98.1
								20	1.121	0.8				1.0		98.2
								22	1.097	39.0				0.2		60.8
								30	1.037	82.7						17.3
9	1220	Kane Co.	Cenomanian	0.43		436	434	Whole		3.7	1.3	0.6	1.7	11.1	3.1	78.5
		Utah, USA.						14	1.226	0.2	0.2		0.2		0.2	99.2
								16	1.194	0.2	0.2		0.2			99.4
								17	1.176	1.5	0.4		0.8			97.3
								18	1.161	6.3	0.4		1.7			91.6
10	892	Cannel City	Westphalian	0.51				Whole		2.7	11	0.9	0.8	3.2	7.6	73.8
		Kentucky, USA.						14	1.230	0.2	3.1			2.5	5.0	89.2
								16	1.204		3.3			0.9	1.1	94.7
								18	1.177	0.4	4.2			0.4	0.8	94.2
								19	1.165	0.4	3.2			0.2	0.6	95.6
								20	1.153	0.9	4.8			0.2	0.2	93.9
								22	1.129	12.6	11.5			0.2		75.7
11	1319	Raleigh Co.	Westphalian	0.55	0.84	443	351	Whole		0.1	12.7	0.1	0.4	7.7	8.5	70.5
		West Virginia						14	1.282					3.7	2.2	94.1
		USA.						16	1.259		0.4			0.8	0.4	98.4
								18	1.235		5.5				0.4	94.1
								20	1.209		28.6				1.0	70.4
								22	1.185		46.3					53.7
								24	1.160	0.8	71.8					27.4
12	1827a	Kanawha Co.	Westphalian	0.56	0.95	448	362	Whole		0.3	11.1		0.2	11.2	10.1	67.1
		West Virginia						10	1.275		0.2			2.4	3.6	93.8
		USA.						12	1.257		0.4			0.6	0.7	98.3
								14	1.240		2.3			1.4	0.4	95.9
								15	1.227		6.5			3.9		89.6
								16	1.202		27.9			1.1		71.0
								18	1.178		75.4					24.6
13	1827b	Kanawha Co.	Westphalian	0.36	0.95	444	409	Whole		4.8	17.3	0.9	1.8	2.6	9.7	62.9
		West Virginia						14	1.257					2.7	0.8	96.5
		USA.						16	1.229		1.0			1.0		98.0
								18	1.202		29.4					70.6
								20	1.174		61.0					39.0
								22	1.148	0.2	92.7					7.1
								24	1.121	0.6	95.1					4.3
14	2123	Linton	Westphalian	0.55		442	357	Whole		2.7	13.8	0.4		6.8	12.9	63.4
		Ohio, USA.						11	1.308						2.1	97.9
								12	1.298						0.4	99.6
								14	1.274		0.2				0.2	99.6
								16	1.256		20.4					79.6
								18	1.225		64.3					35.7
								20	1.198		94.9					5.1
15	2067	Melville Island	Devonian	0.62		449	579	Whole			64.9			33	0.3	1.8
		Canada						9	1.327					100.0		
								11	1.303		0.2			99.8		
								12	1.291		1.2			98.8		
								18	1.212		97.7			2.3		
								20	1.187		99.2			0.8		
								22	1.160		99.2			0.8		

Fig. 1. Summary of the petrographic data of the 15 torbanites and cannel coals. Torbanites are arranged in order of decreasing alginite content, while cannel coals are in order of decreasing groundmass percentage. Rock-Eval Hydrogen Index values are posted for each sample on the left side of the diagram (nd: data not available).

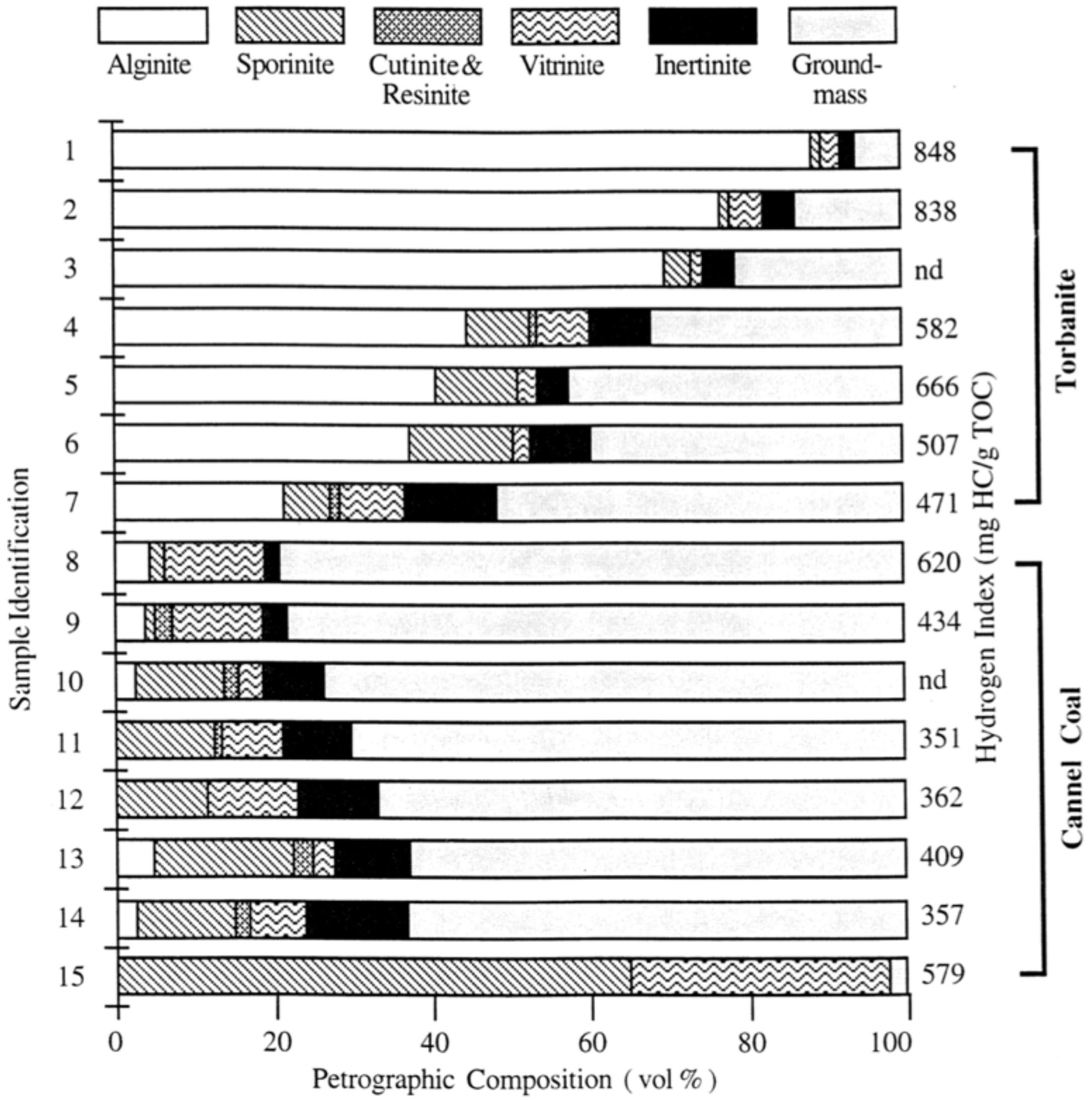

Fig. 2. Density gradient profiles of torbanites and cannel coals. Numbered fractions were examined petrographically (Table 1).

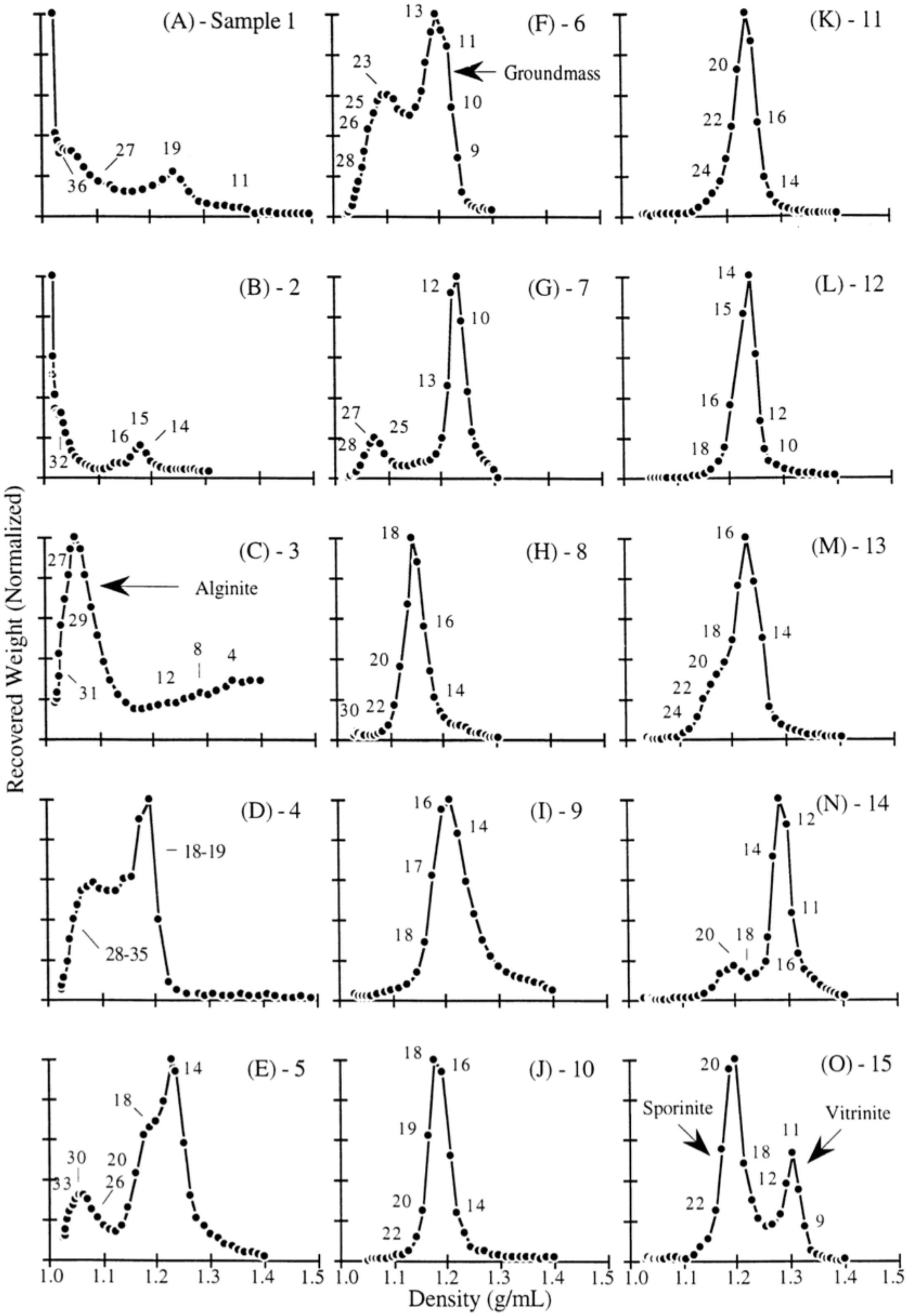

Fig. 3. Density distribution of the varieties of macerals and groundmass from torbanite and cannel coal, showing a shift towards higher density from alginite, sporinite to vitrinite, and from lamalginitic to vitrinitic groundmass.

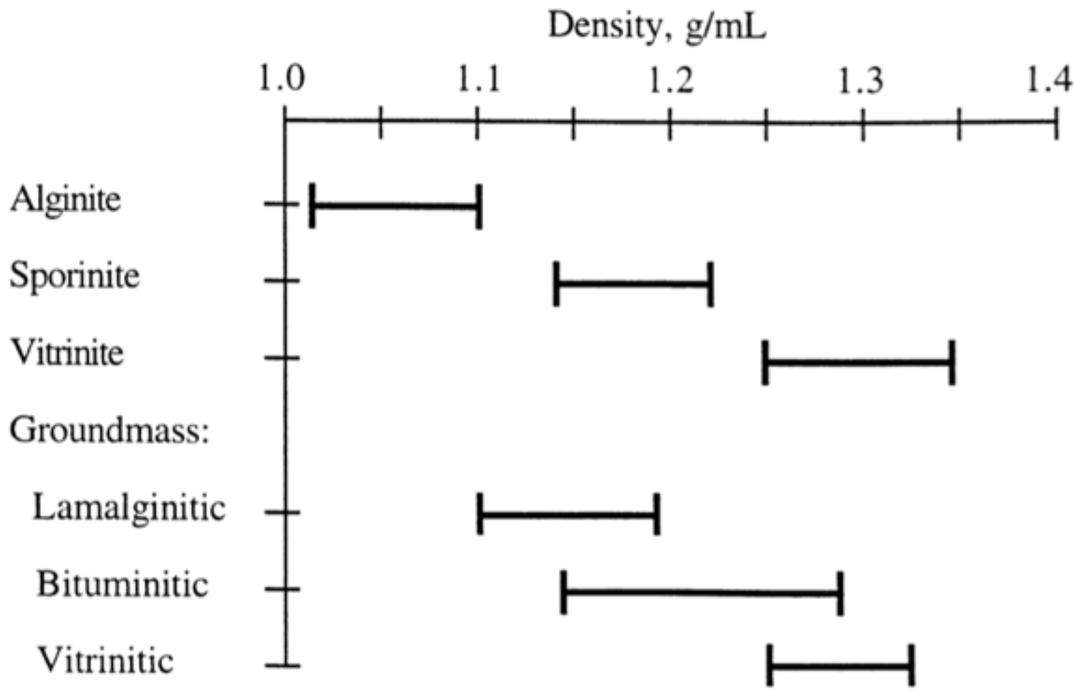

Plate 1. Representative photomicrographs (reflected light; oil immersion). 50 µm scale bar applies to all.
A - Torbanite (sample 1), showing a predominance of *Reinschia* alginite (notice the strong internal reflection of the alginite). The greenish gray particle is degraded vitrinite. Alpha, Australia, Permian. Perpendicular to bedding, white light.
B - Alginite concentrate (sample 1, fraction 39 in Table 1), blue light. Notice the greenish fluorescence of the mounting medium.
C - Degraded vitrinite concentrate (sample 1, fraction 19), white light.
D - Torbanite (sample 2), showing a predominance of *Reinschia* alginite with well-preserved cell structure. Groundmass shows a weak, dark brown fluorescence and no microlamellae. Middle River, NSW, Australia, Permian. Oblique to bedding, blue light.
E - Alginite concentrate (sample 2, fraction 38) with a yellowish fluorescence, blue light.
F - Bituminitic groundmass concentrate (sample 2, fraction 15), displaying a brownish red fluorescence, blue light.
G - Cannel (sample 8), dominated by a lamalginitic groundmass made up of densely-compacted fluorescing lamellae. Also notice the brightly fluorescing *Pila* alginite and the weekly fluorescing vitrinite stringers. Breckinridge, Kentucky, USA, Westphalian. Perpendicular to bedding, blue light.
H - Alginite concentrate (sample 8, fraction 30), displaying a bright yellowish fluorescence, blue light.
I - Lamalginitic groundmass concentrate (sample 8, fraction 18), showing a layered texture and brownish yellow fluorescence, blue light.
J - Cannel (sample 13), yellow fluorescing sporinite and *Pila* alginite set in a reddish brown groundmass with many microlamellae. The dark particles are inertinite. Kanawha County, West Virginia, USA, Westphalian. Perpendicular to bedding, blue light.
K- Sporinite concentrate (sample 13, fraction 24), blue light.
L - Groundmass concentrate (sample 13, fraction 16), blue light.

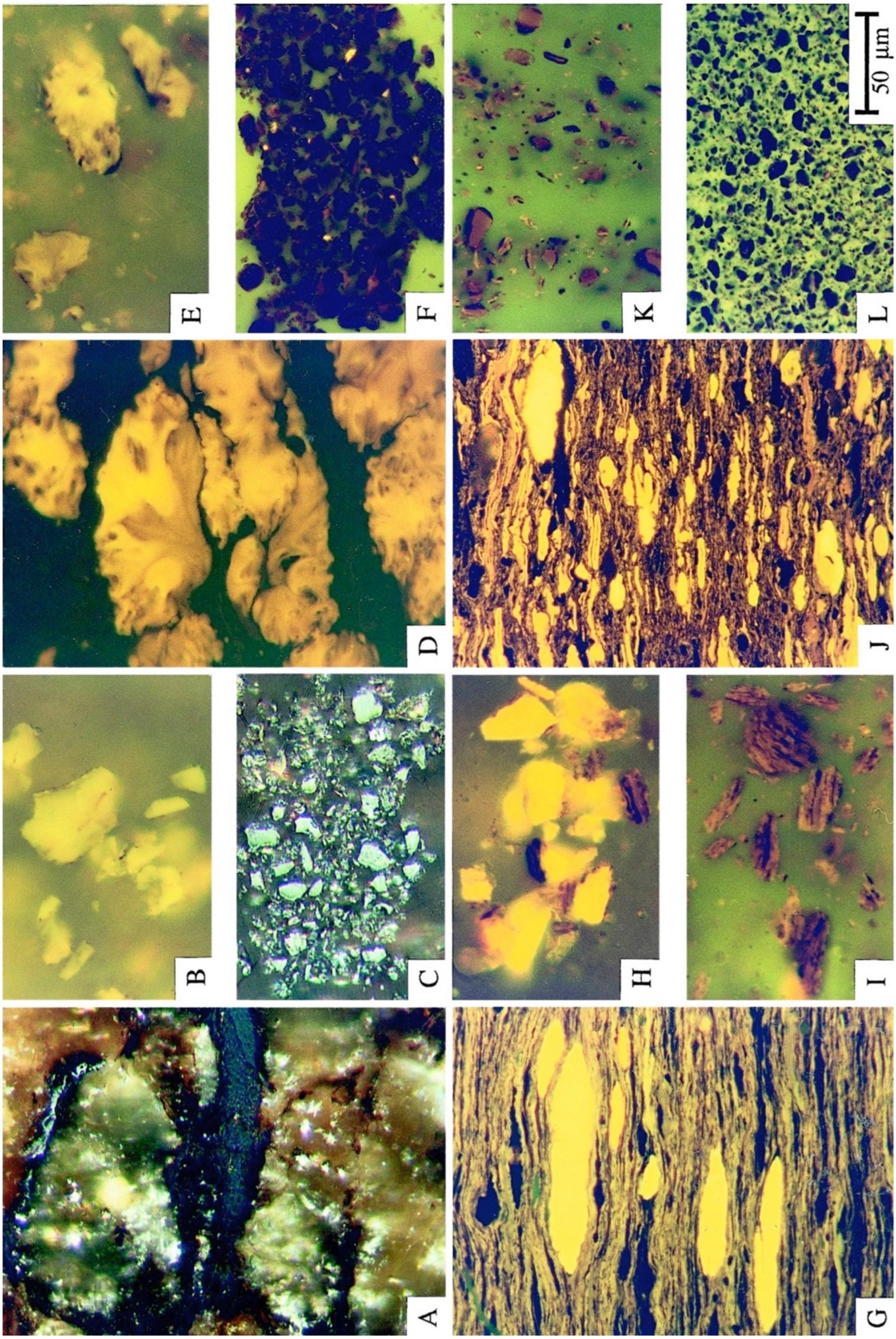

Plate 1

Plate 2. Representative photomicrographs (reflected light; oil immersion). 50 µm scale bar applies to all , except 2A, which uses the 20 µm scale bar.
A - Cannel (sample 10), showing a predominance of a reddish groundmass which is seen to be brightly fluorescing microlamellae (yellow, 2-3 µm) set in an amorphous organic matter. Also notice the bright yellow *Pila* alginite(near bottom), sporinite(top) and dark inertinite. Cannel City, Kentucky, USA, Westphalian. Perpendicular to bedding, blue light.
B - Cannel (sample 11), showing various types of maceral particles set in a fine-grained whitish gray groundmass dominated by micrinite. Raleigh County, West Virginia, USA, Westphalian. Perpendicular to bedding, white light.
C - Sporinite concentrate (sample 11, fraction 24), showing a yellowish brown fluorescence, blue light.
D - Groundmass concentrate (sample 11, fraction 16), showing a predominance of micrinite, white light.
E - Cannel (sample 14), brightly yellow fluorescing sporinite and *Pila* alginite set in a weakly fluorescing vitrinitic groundmass. Linton, Ohio, USA, Westphalian. Perpendicular to bedding, blue light.
F - Sporinite concentrate (sample 14, fraction 20), blue light.
G - Vitrinitic groundmass concentrate (sample 14, fraction 12), showing a weak reddish fluorescence, blue light.
H - Spore Cannel (sample 15), showing a predominance of sporinite (dark gray). Also notice the gray vitrinite particles and white inertinite. Melville Island, Canada, Devonian. Perpendicular to bedding, white light.
I - Sporinite concentrate (sample 15, fraction 22), blue light.
J - Vitrinite concentrate (sample 15, fraction 11), white light.

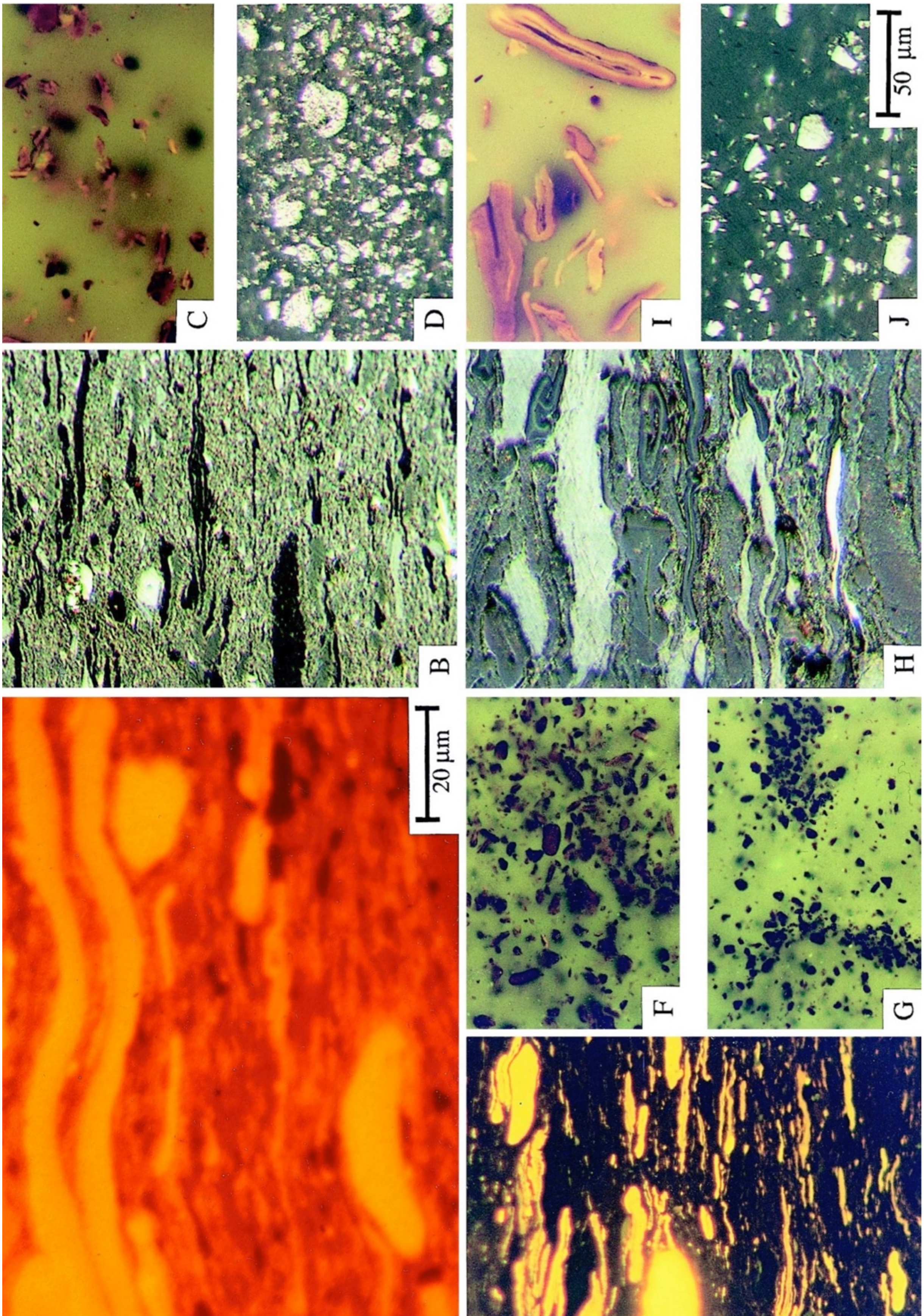

Plate 2